... Engineering Conference
and Exhibition New York, New York
August 9-13, 1987

NAG 1-489
IN 37-CR
270017
6P

THE ACCELERATION MAP AND ITS USE IN MINIMUM TIME MOTION PLANNING OF ROBOTIC MANIPULATORS

Zvi Shiller
Steven Dubowsky

Department of Mechanical Engineering
Massachusetts Institute of Technology
Cambridge, MA 02139

ABSTRACT

A method to approximate time optimal paths for robotic manipulators is presented. The method uses the Acceleration Map which is a graphical representation of the manipulator dynamics. The Acceleration Map is composed of Acceleration Lines that represent the directions of maximum tip acceleration from a point at zero velocity. The time optimal path is approximated by connecting a smooth curve between the end points, tangent to the Acceleration Lines. It is shown that nonsingular time optimal paths, with zero velocity at their end points, are tangent to one of the Acceleration Lines near the end-points.

INTRODUCTION

The task of obtaining the time optimal motion for robotic manipulators with nonlinear and coupled dynamics, using existing methods [1-5], is computationally cumbersome, and typically done off-line. In applications where off-line methods are not acceptable, a fast approximation to the optimal motion is desirable. In this paper, the motion of a manipulator between two end points is regarded as being composed of a path, describing the locations (and orientation) of the end-effector, and a velocity profile along that path. The optimal motion is, therefore, composed of the optimal path and the optimal velocity profile along that path. This paper presents a computationally fast method that can obtain approximations to time optimal paths, and is potentially applicable to on-line path planning. The motion along the path is obtained using the method for time optimal motion along specified paths, presented in References [6,7]. The path approximation method is based on a graphical representation of the acceleration capabilities of the manipulator. Graphical representations of manipulator dynamics have been previously developed in the form of the effective inertia of the manipulator tip [8], its dynamic manipulability [9], and its acceleration capabilities [10]. The acceleration capabilites of the manipulator tip, in the form of Acceleration Parallelograms, were first used for optimal kinematic design of manipulators [11]. In [10] the Acceleration Hyperparallelepipeds were introduced, which are similar to the Acceleration Parallelograms, but generalized to higher dimensions.

The method presented here introduces the Acceleration Parallelepipeds which represent the maximum acceleration capabilities of the end-effector in all directions from a given point. The Acceleration Parallelepipeds are similar to Khatib's Acceleration Hyper- parallelepipeds, except that here they represent the acceleration component parallel to the direction of motion, while Khatib's Acceleration Hyperparallelepipeds represent the absolute tip acceleration. The Acceleration Parallelepipeds are used to construct the Acceleration Lines that indicate the directions in which a manipulator tip has the highest acceleration from a given point in the work-space, starting with zero velocity. It is shown here that nonsingular minimum time paths are tangent to the Acceleration Lines at the end points. Near-optimal paths can be constructed by connecting smooth curves between the end points, tangent to the Acceleration Lines. Time optimal paths, obtained with a more accurate off-line method, presented in [12], are shown to be highly correlated with the Acceleration Lines. The method is derived in a general form for any nonredundant manipulators, however, it can be visualized easily in two dimensions, as demonstrated in examples for a two link manipulator. The Acceleration Lines provide also insights into the possible shape of the time optimal paths, and can be used as a design tool in the design of work cell layouts for fast motion between work stations.

THE METHOD

A manipulator's tip acceleration capabilities are represented graphically by the Acceleration Lines (AL) which represent the directions in which the manipulator's tip can move with the highest

from the Acceleration Parallelepipeds (AP) which represent the maximum available acceleration of the manipulator tip in all directions at a given configuration. This method is applicable to manipulators with rigid links for which the dynamic model and joint coordinates can be defined for any point on the path

The Acceleration Parallelepiped

In this section the Acceleration Parallelepipeds (AP) are presented. An AP, derived from the manipulator dynamics, represents the maximum acceleration available for the manipulator tip in all directions from a given point in the work space. The acceleration represents the component in the direction of motion (tangent to the path) of the absolute acceleration, and is dependent on the velocity and path curvature.

To obtain the Acceleration Parallelepipeds we first consider the equations of motion of the manipulator:

$$M\ddot{\underline{\theta}} + \dot{\underline{\theta}}^T C\,\dot{\underline{\theta}} + \underline{G} = \underline{T} \qquad (1)$$

where M is an nxn inertia matrix, n is the number of the manipulator degrees-of-freedom, C is an nxnxn array of the coefficients of the coriolis forces, $\underline{G}$ is a vector of the gravity forces, $\underline{T}$ is the vector of actuator efforts, and $\underline{\theta}$, $\dot{\underline{\theta}}$ and $\ddot{\underline{\theta}}$ are the joint displacements, velocities and accelerations, respectively [6,7]. The actuator torques are bounded by constant bounds:

$$T_{imin} < T_i < T_{imax}; \qquad i = 1,\ldots n \qquad (2)$$

The path of the end-effector can be represented by the six dimensional vector $\underline{P}$, composed of the position and orientation of the end-effector:

$$(\underline{X}, \underline{\varphi}) = (x,y,z,\varphi_1,\varphi_2,\varphi_3)$$

where $\underline{X}$, is the position vector, and $\underline{\varphi}$ is the vector of the Euler angles, representing the orientation of the end-effector fixed frame with respect to an inertial frame. The mapping from the joint angles to work space coordinates is defined by the kinematic transformation:

$$\underline{P}(S) = \underline{R}(\underline{\theta}) \qquad (3)$$

If the displacement S is a parameter along the path, the vectors $\dot{\underline{S}}$ and $\ddot{\underline{S}}$ are the velocity and the acceleration tangent to the path, with the magnitudes $\dot{S}$ and $\ddot{S}$, respectively. Differentiating Equation (3) twice with respect to time and solving for $\dot{\underline{\theta}}$ and $\ddot{\underline{\theta}}$ yields [7]:

$$\begin{aligned} \dot{\underline{\theta}} &= R_\theta^{-1}\,\underline{P}_s\,\dot{S} \\ \ddot{\underline{\theta}} &= R_\theta^{-1}\{\underline{P}_s\ddot{S} + \underline{P}_{ss}\,\dot{S}^2 - (R_\theta^{-1}\underline{P}_s)^T R_{\theta\theta}\,(R_\theta^{-1}\underline{P}_s)\,\dot{S}^2\} \end{aligned} \qquad (4)$$

where R_θ is the Jacobian matrix:

$$R_\theta(i,j) = \partial R_i/\partial\,\theta_j$$

and $R_{\theta\theta}$ is the Hessian of the vector function $\underline{R}$. $\underline{P}_s$ is a unit vector in the direction of motion, $\underline{P}_{ss}$ is a vector in the direction of the centrifugal acceleration. The s and θ subscripts denote partial derivatives with respect to the scalar S and the vector $\underline{\theta}$, respectively. Substituting Equation (4) into Equation (1) yields the equations of motion in terms of , $\dot{S}$ and $\ddot{S}$:

$$M^*\ddot{S} - b\,\dot{S}^2 - G = T \qquad (5)$$

where

$$M^* = M\,R_\theta^{-1}$$

$$b = MR_{\theta\theta}\cdot^{-1}\{\underline{P}_{ss} - (R_\theta^{-1}\underline{P}_s)^T R_{\theta\theta}(R_\theta^{-1}\underline{P}_s)\} + (R_\theta^{-1}\underline{P}_s)^T C(R_\theta^{-1}\underline{P}_s)$$

Solving Equation (5) for the acceleration $\ddot{S}$ yields:

$$\ddot{S} = R_\theta\,M^{-1}(T - b\,\dot{S}^2 + G) \qquad (6)$$

If we ignore the gravity forces $\underline{G}$ and assume zero velocity, then Equation (6) reduces to:

$$\ddot{S} = R_\theta\,M^{-1}\,T \qquad (7)$$

For given joint angles $\underline{\theta}$, Equation (7) defines a linear mapping from the actuator torques $\underline{T}$ to the acceleration $\ddot{S}$ at zero velocity. In multi-dimensional space, this transformation maps the rectangular polyhedron, representing the region of the available torques $\underline{T}$, to the Acceleration Parallelepipeds (AP). In two dimensions, the parallelepipeds reduce to parallelograms, as shown in Figure 1. The AP defines the region of the maximum available acceleration in all directions at a given configuration. Referring to Figure 1, the maximum acceleration is given by the vector directed in the direction of motion, originating at the AP center. The magnitude of the vector from the AP center to the AP boundaries determines the magnitude of the available acceleration in this direction. Similarly, the maximum deceleration is given by the vector from the AP center directed in the opposite direction.

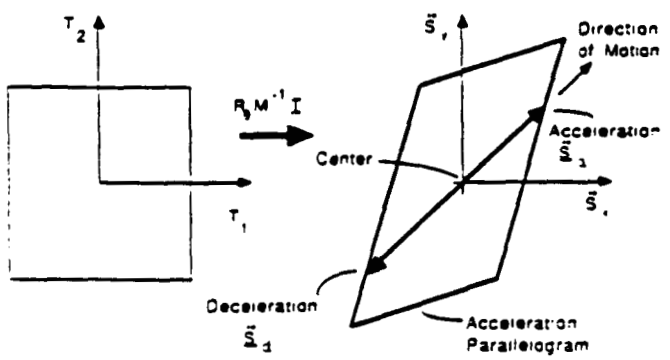

Figure 1 Mapping the Actuator Torques into the Acceleration Parallelogram at Zero Velocity.

Plotting the AP in the work space provides insights into the acceleration capabilities of the manipulator. Figure 2 shows the Acceleration Parallelograms in work space and in joint space coordinates for the two link manipulator shown in Figure 3 with the parameters given in Table 1. Note that in joint space the Acceleration Parallelograms are uniform in the θ_1 direction since the equations of motion are not a function of θ_1 for this system. From Figure 2 it can be seen that the maximum end-effector acceleration varies with the direction of motion and with the location of the tip in the work space. It is possible to obtain a desired manipulator dynamic performance, such as isotropic and uniform sized Acceleration Parallelograms, by

optimizing ... the manipulator's parameters [9]. These Acceleration Parallelepipeds were obtained at zero velocity; however, unlike the Acceleration Hyperparallelepipeds presented in [10], here, the Parallelepipeds deform and lose their shape as the velocity increases, as shown in [12].

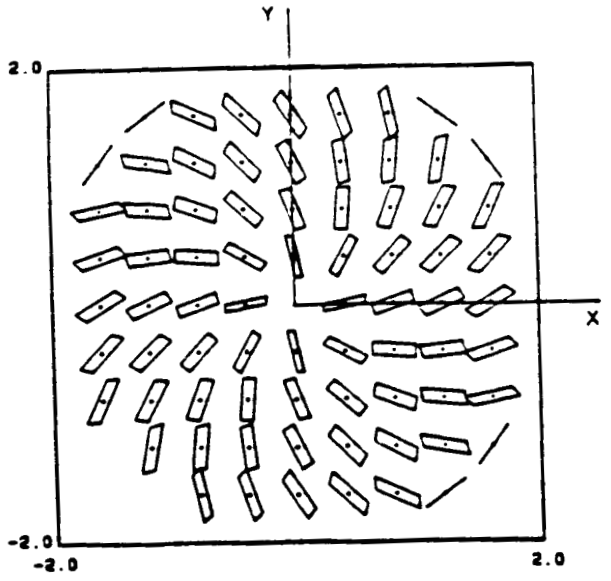

a) The Acceleration Parallelograms in Work Space Coordinates

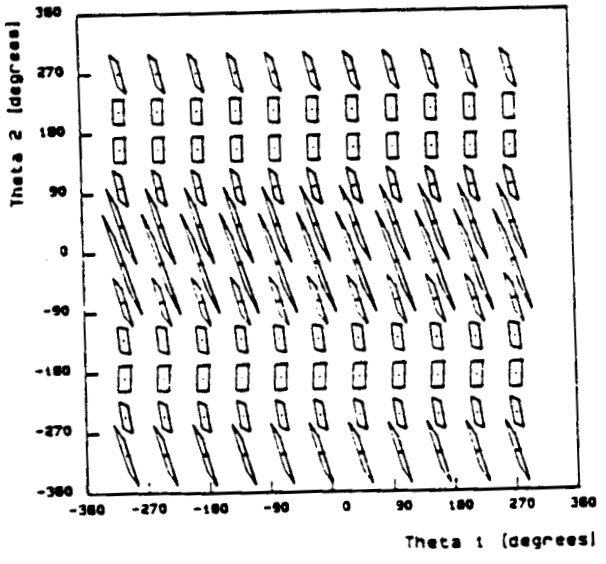

b) Acceleration Parallelograms in Joint Space Coordinates

Figure 2 Acceleration Parallelograms for the Two Link Manipulator Shown in Figure 3

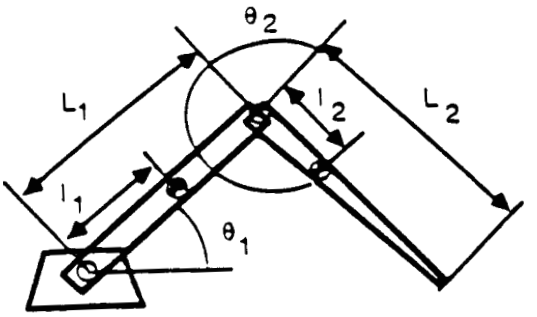

Figure 3 A Two Link Manipulator

l_1 = 0.5 m.	L_1 = 1.0 m.	m_1 = 1 kg	I_1 = .2 Kg-m^2	T_1 = 10 N-m
l_2 = 0.5 m.	L_2 = 1.0 m.	m_2 = 1 kg	I_2 = .2 Kg-m^2	T_2 = 10 N-m

Table 1 Manipulator's Parameters

The Acceleration Lines

At zero velocity, the Acceleration Lines (AL) represent the directions of motion with the highest acceleration of a manipulator's tip from a given point. These lines reflect the manipulator's specific parameters and its dynamic behavior in the work space. The AL can be derived either in work space or in joint space coordinates; in either representation, they can be used to suggest the general shape of time optimal paths.

An Acceleration Line is constructed by plotting the locations of a vertex of the Acceleration Parallelepipeds, following successive moves in the direction of that vertex, as shown in Figure 4 schematically for a two-dimensional manipulator. Since, in general, the AP are shaped differently at different points in the manipulator space, the assembly of the line segments results in a curved line that reflects the change in direction of the manipulator's maximum acceleration capabilities. Since each Acceleration Parallelepiped has n vertices, there are n different AL departing from each point, n being the number of the manipulator's degrees of freedom. Since the AP with zero velocity is used at all points along the AL, these lines are most meaningful when the velocity is relatively small.

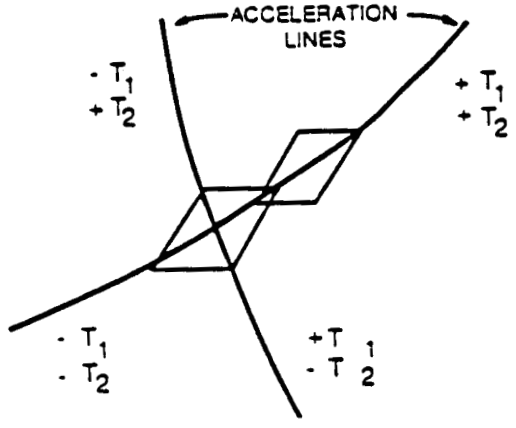

Figure 4 The Construction of The Acceleration Lines

Acceleration Lines and Time Optimal Paths

It is shown below that *nonsingular* and *bang-singular-bang* time optimal paths are tangent to the Acceleration Lines at the end points. A *nonsingular* optimal path is defined here as a path along which the time optimal trajectory (path and velocity) consists of *bang-bang* control (the actuators are at their extremes at all times). A *singular arc* is a portion of a time optimal trajectory which is not necessarily *bang-bang*. A *bang-singular-bang arc* is a time optimal trajectory with *bang-bang* control only near the end points.

Corollary

Nonsingular and *bang-singular-bang* time optimal paths are tangent to the Acceleration Lines at the end points, provided the velocity at the end points is zero.

Proof

By definition, the actuators of *nonsingular* and *bang-singular-bang* trajectories are at their extremes at least near the end points. The Acceleration Lines are constructed such that they depart from the end points in the directions obtained by applying some combination of the actuator extremes (the actuator extremes represent the vertices of the $\mathcal{I}$ region which are mapped into the vertices of the AP). Hence, an optimal path tangent to one of the Acceleration Lines near the end points is either *bang-bang* or *bang-singular-bang*, assuming zero velocity at the end points.

The Acceleration Lines provide partial information about the shape of time optimal paths near their end points. For nonlinear systems, several local time optimal paths may exist which satisfy this corollary [2], each tangent to a different set of Acceleration Lines. Theoretically, if there are n Acceleration Lines at every point in the work space, there may be at most $(2n)^2$ different *nonsingular* local time optimal paths. Experience shows that the global optimal path is the shortest one among all the local optimal ones [12].

Approximate time optimal paths can be obtained by connecting the end points with smooth curves, tangent to the Acceleration Lines. The optimal motion along these paths is then obtained using the method presented in [6,7]. These paths are only approximations to the true time optimal paths since their shape further away from the end points is not known exactly. The shape of the optimal paths between the end points depends on the size of the coriolis forces, the vector $\underline{b}$ in Equation (5); the smaller the coriolis forces, the closer the path to the Acceleration Lines. Approximating the shape of the optimal path, in particular its slopes at the end points, may speed up exact optimization methods, such as the one using the Pontryagin maximum principle [2], and other methods which require an initial path for the optimization [1].

EXAMPLES

The following examples demonstrate the high corellation between the Acceleration Lines and time optimal paths, obtained with the method presented in [1]. In the following examples, the two link manipulator shown in Figure 3 is used.

Figure 5 shows the manipulator and the Acceleration Lines at the end points. The time optimal path, also shown in Figure 5, was obtained by the parameter optimization method [1], representing the path by 7 B splines. The optimal path in Figure 5 is shown to be consistent with the Acceleration Lines, suggesting that this path is indeed close to the true optimal path. Optimal paths obtained with more control points tended to come closer to the Acceleration Lines.

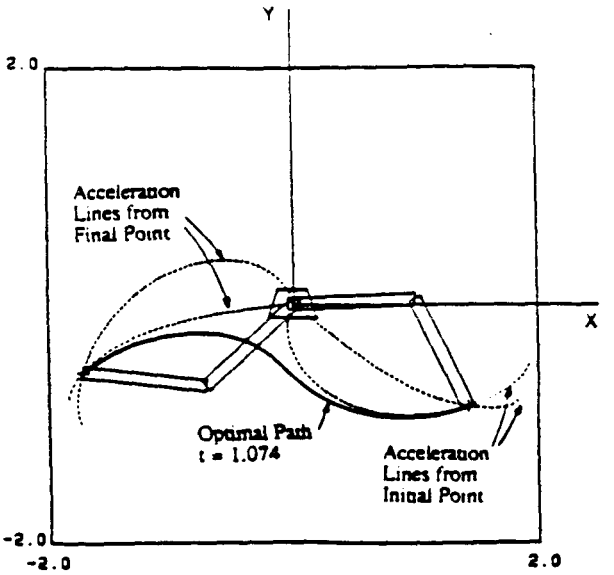

Figure 5 The Time Optimal Path and the Acceleration Lines

Figure 6 shows two optimal paths with similar times. Plotting the Acceleration Lines at the end points, shown in Figure 7, suggests that at least two global anti-symmetric solutions can be expected. These paths were obtained while optimizing in work space coordinates. While optimizing in joint space coordinates, the optimal path shown in Figure 8 was obtained. Again, comparing the path to the Acceleration Lines may explain or even suggest its shape. The differences between the work space and joint space optimizations arise from the fact that while optimizing the path in work space coordinates, the solutions tend to avoid the center point which is a point of singularity. In joint space representation, there are no singular points, therefore the solution can pass through the center point, as was shown in Figure 8. The second symmetric solution in joint space coordinates is a mirror image of the path shown in Figure 8. In joint space, the two solutions were obtained by optimizing two separate paths, with one common end point, and the other end points spaced 360 degrees apart, as shown in Figure 9. Also shown in Figure 9 are the joint space Acceleration Lines at the end points. Figures 10 and 11 show optimal paths and their Acceleration Lines between other end points.

These examples demonstrate that optimal paths are tangent to the Acceleration Lines at the end points. The high correlation between time optimal paths and Acceleration Lines suggests that the general shape of the optimal paths could be predicted from the shape of the Acceleration Lines only. Experience shows that the global optimal path is the shortest path among all possible local optimal paths (tangent to one of the Acceleration Lines at the end points).

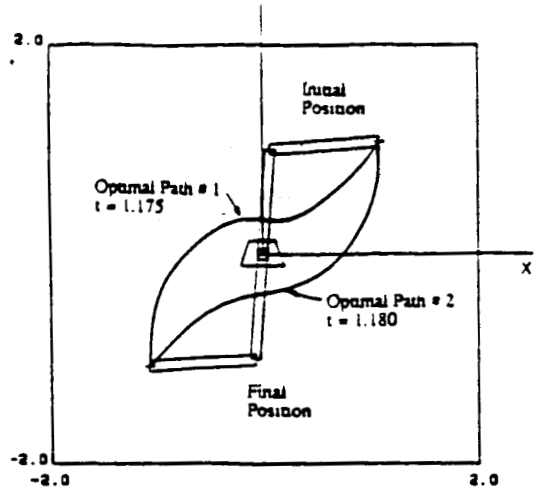

Figure 6 Two Symmetrical Optimal Paths Optimized in Work-Space Coordinates

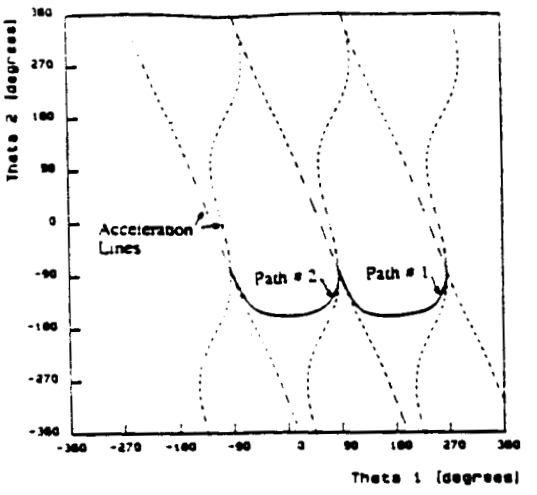

Figure 9 The Optimal Paths from Figure 7 Shown in Joint Space Coordinates with the Acceleration Lines

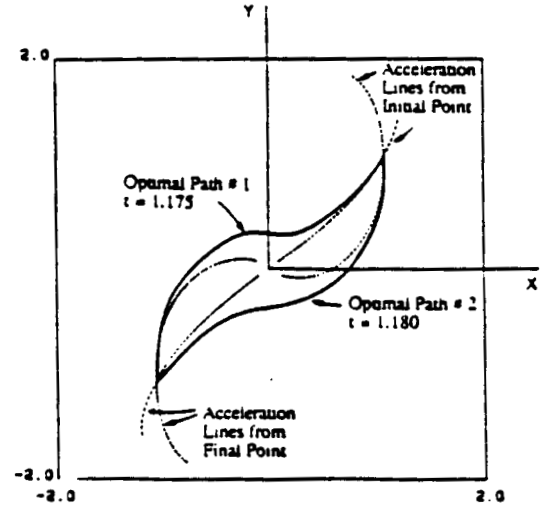

Figure 7 The Acceleration Lines for the Optimal Paths from Figure 6

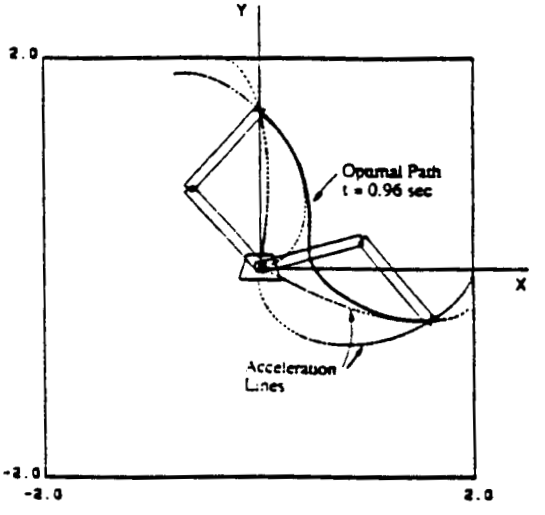

Figure 10 An Optimal Path and the Acceleration Lines

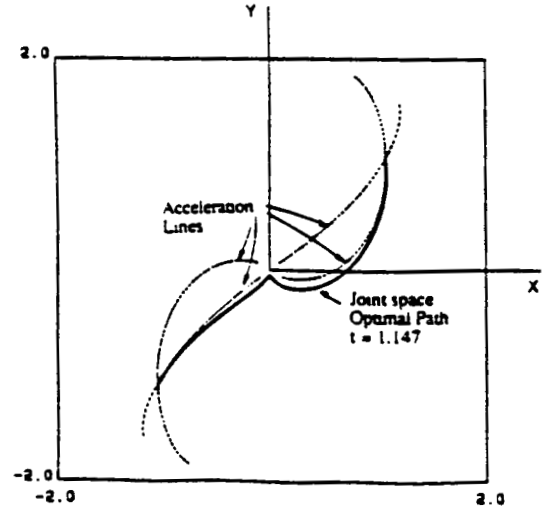

Figure 8 An Optimal Path Shown in Work Space Coordinates, Optimized in Joint Space Coordinates for Same End Points as in Figure 6

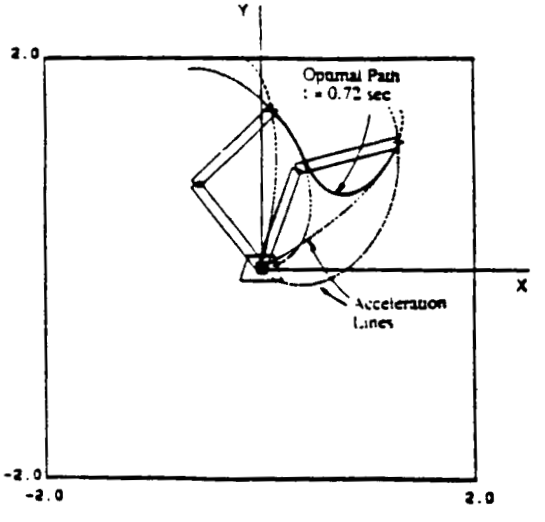

Figure 11 An Optimal Path and the Acceleration Lines

CONCLUSIONS

A heuristic method to analyze optimal paths and synthesize near-minimum paths has been presented. The method uses Acceleration Lines to represent the directions of maximum acceleration of a manipulator tip in work space or joint space coordinates. It is shown that *nonsingular* time optimal paths are tangent to the Acceleration Lines at the end points, provided that the initial and final velocities are zero and that he coriolis forces are relatively small. Examples are presented that demonstrate the close fit between time optimal paths and their Acceleration Lines. The examples and experience suggest that the global optimal path, without obstacles, is the shortest path among the local optimal ones. This path can be easily approximated using the Acceleration Lines only.

Since the Acceleration Lines are obtained by a direct computation, they can be used to generate quickly near-minimum paths in a real time path planning procedure. Approximations to time optimal paths can be also used as initial conditions for more exact optimization procedures, such as the ones presented in [1,2,5]. The Acceleration Lines provide insights into a manipulator's dynamic behavior, and can be used for work cell layout design.

ACKNOWLEDGMENTS

The support of this research by the Automation Branch of NASA Langley research Center under Grant NAG-1-489 is acknowledged.

REFERENCES

1. Dubowsky, S., Norris, M.A., and Shiller, Z., "Time Optimal Path Planning for Robotic Manipulators with Obstacle Avoidance: A CAD Approach," Proceedings of 1986 IEEE International Conference on Robotics and Automation, San Francisco, CA., March 1986.

2. Geering, H., Guzzella, L., Hepner, S.A.R., and Onder, C.H., 1986, "Time-Optimal Motions of Robots in Assembly Tasks", IEEE Transactions on Automatic Control, Vol. AC-31, No. 6, June 1986, pp. 512-518.

3. Kahn M. E. and Roth B., 1971, "The Near-Minimum-Time Control of Open-Loop Articulated Kinematic Chains," Journal of Dynamic Systems, Measurement and Control, Vol. 93, No. 3, Sept. 1971, pp. 164-172.

4. Sahar, G. and Hollerbach, J.M., 1985, "Planning of Minimum-Time Trajectories for Robot Arms," Proceedings of the IEEE International Conference on Robotics and Automation, pp. 751-758, St. Louis, Mo., March, 1985.

5. Weinrab, A. and Bryson, A.E., 1985, "Optimal Control of Systems With Hard Control Bounds," Proceedings of The 1985 American Control Conference, Boston, MA., pp. 1248-1252, June 1985.

6. Bobrow, J.E., Dubowsky, S., and Gibson, J.S., "Time-Optimal Control of Robotic Manipulators," The International Journal of Robotics Research, Vol. 4, No. 3, 1985.

7. Shiller, Z., and Dubowsky, S., "On the Optimal Trajectories for Robotic manipulators with Actuators and End-Effector Constraints," Proceedings IEEE International Conference on Robotics and Automation, St. Louis, March 1985

8. Asada, H., "A Geometrical Representation of manipulator Dynamics and Its Application to Arm Design," ASME J. of Dynamic Systems, Measurment and Control, Sept 1983, Vol. 105, No. 3, pp. 131-135.

9 Yoshikawa, T., "Dynamic manipulability of Robot Manipulators." Proc. 1985 IEEE International Conference on Robotics and Automation, St. Louis, March 1985, pp. 1033-1038.

10. Khatib, O., "The Operational Space Formulation in the Analysis, Design, and Control of Robot Manipulators," Proceedings of Third International Symposium of Robotics Research, Gouvieux, France, October 1985

11. Fraize G., Vertut J. and Hugon R., 1985, "Coverage Optimization of Articulated Manipulators", in *Theory and Practice of Robots and Manipulators*, pp. 351-361, Kogan Page, London 1985, MIT Press 1985.

12. Shiller, Z., "Time Optimal Motion Planning for Robotic Manipulators," Doctoral Thesis, Massachusetts Institute of Technology Cambridge MA, June 1987.